On the Orientation of Grid Systems for the Statistical Prediction of Tropical Cyclone Motion

LLOYD J. SHAPIRO

Atlantic Oceanographic and Meteorological Laboratory, NOAA, Hurricane Research Division, Miami, FL 33149

CHARLES J. NEUMANN

National Hurricane Center, NWS/NOAA, Coral Gables, FL 33146

(Manuscript received 29 January 1982, in final form 8 August 1983)

ABSTRACT

Statistical models for the prediction of tropical cyclone motion traditionally have been formulated in a coordinate system oriented with respect to zonal and meridional directions. An investigation is made here into the forecast error reducing potential of a grid system reoriented with respect to initial storm heading. The developmental data comprise Atlantic forecast situations from 1965 through 1980 on all storms initially north of about 25°N. Reorientation of the coordinate system reduces the total variance in 24 h storm motion by 40%, projects most of the motion onto one (along-track) component of displacement, and makes the components nearly independent of each other. For 48 and 72 h displacements, however, these advantageous effects are substantially diminished or eliminated.

Synoptic predictors derived from current deep-layer mean heights on a grid of 1700 km radius are used to forecast storm displacements. For the developmental data, grid reorientation lowers the 24 h forecast error by 13%, and reduces the slow speed bias by a factor of ⅓. For 24 h forecasts the skill in the prediction of cross-track motion is small. Empirical Orthogonal Function and Principal Estimator Patterns provide insight into the role of reorientation in the reduction of forecast error, and the position of grid-point height predictors selected by a screening technique.

1. Introduction

a. Current forecast methodology

The attributes of the various statistical and numerical tropical cyclone track prediction models used operationally at the National Hurricane Center (NHC) are described by Neumann and Pelissier (1981). The grid system historically used in the development of statistical models throughout the decades of the 1960s and the 1970s moves with the storm, is always oriented in the zonal-meridional sense, and contains a rather coarse grid-spacing. Neumann and Lawrence (1975), who describe NHC's current statistical-dynamical model, known as NHC73, illustrate such a grid (their Fig. 3). Typically, gridded 1000, 700, and 500 mb geopotential height fields and, more recently, deep-layer-mean height fields, are utilized to represent the synoptic state. Step-wise screening regression techniques are employed to select predictors or predictor functions (i.e., gradients, thicknesses, time changes) that are statistically related to tropical cyclone motion. Additional predictors, important principally for the shorter range projections, are derived from climatology and persistence.

Although tropical cyclone motion is a vector quantity, zonal and meridional components of storm motion are forecast separately and independently. These are then combined to give a prediction of the vector displacement, ignoring any correlation that may exist between components.

b. The steering concept

The steering principle for tropical cyclone motion assumes that the storm moves in accordance with the environmental current in which it is embedded. Thus, the large-scale geopotential height contours and winds in the vicinity of the storm will be oriented more or less along the storm heading which, in general, is not along either axis in the geographically fixed coordinate system. Indeed, Fig. 1 shows that, most of the time, tropical cyclone motion over the Atlantic basin tends to be *between* the zonal and meridional axes. There is a bimodal distribution, with storms predominantly moving toward the west-northwest before recurvature or toward the northeast after recurvature.

Earlier authors (e.g., George and Gray, 1976 and Chan *et al.* 1980) have used a grid system oriented with respect to the direction of cyclone movement to relate the motion to surrounding wind and temperature fields. Statistical forecast models presently use components of current and past storm motion directly as

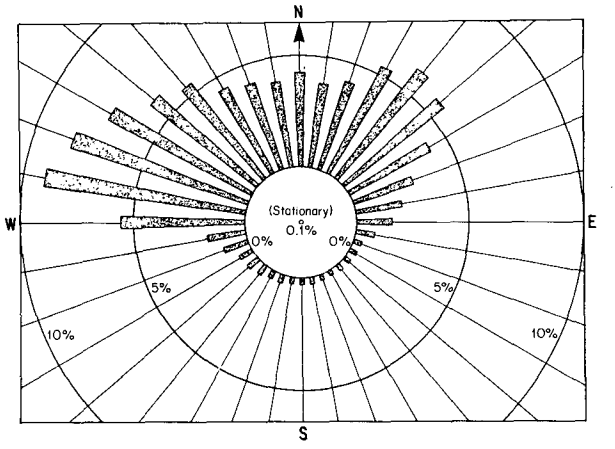

FIG. 1. Distribution of initial storm headings for 23 285 cases from 1886–1981. Length of bars gives percent of cases falling within 10° angular segments. Average storm heading is 338° (west of north).

a (persistence) predictor of future motion, but do not take advantage of the natural orientation of height and wind fields relative to the motion. In fact, as noted by Neumann (1978), statistical screening techniques invariably select present and past storm motion as predictors of short-range tropical cyclone displacement over steering predictors derived from the surrounding flow. This circumstance is partly due to the deficiency and poor quality of the data, particularly at midlevels, in the vicinity of tropical storms. It is also partly due, in our opinion, to an inadequate grid structure for representing data fields. This topic is the subject of the present paper.

It has been particularly difficult to effect much improvement in the 24 h forecast errors, which declined only 14% over the 27-year period 1954–1980 (Neumann, 1981). Thus, any new technology that could aid in further reduction in forecast error is clearly important. Given the present data inadequacies, it is especially important to fully utilize available synoptic data. Any increase in the variance-reducing potential of synoptic predictors alone would render these data more competitive with climatology and persistence for short-range forecasts, and likely offer additional independent information.

c. *Outline of paper*

In the course of development of a revised operational statistical-dynamical forecast model for the Atlantic basin, we have tested the potential of a grid system reoriented with respect to storm heading. We are here concerned only with predictors derived from current synoptic height data. In Section 2, the deep-layer-mean height predictors, the grid system and the method of grid rotation used in this study are described. Section 3 relates the grid rotation to the distribution of storm displacement vectors. The differences in forecast errors and speed biases between the geographically and storm heading-oriented coordinate systems are quantified in Section 4 using a step-wise screening technique. Empirical Orthogonal Function (EOF) and Principal Estimator Pattern (PEP) analyses in Section 5 provide insight into the role of rotation in the improvement of track forecasts, as well as the position of the grid-point predictors derived from screening. Section 6 summarizes the results and discusses their application in operational models.

2. Description of height data and rotation of grids

As noted by Miller and Moore (1960), and previous authors, the motion of a tropical cyclone is largely determined by forces integrated through a deep layer and over a substantial area surrounding the storm. Deep-layer winds have been used successfully to forecast storm motion in barotropic numerical prognostic models (e.g., Sanders *et al.*, 1975). In the present study we use pressure-weighted deep-layer-mean geopotential height predictors interpolated from National Meteorological Center (NMC) operational analyses at all 10 standard levels from 1000 to 100 mb. For convenience, height departures from normal (Jordan's September mean) are substituted. The use of the deep-layer heights takes advantage of upper (cirrus) and lower (cumulus) satellite winds, and avoids sole reliance on the data-deficient 500 mb level (Neumann, 1981). The grid on which the height predictors in the present study are defined is shown oriented with respect to geography in Fig. 2. The storm-centered grid has a uniform 278 km spacing, along longitude and latitude circles. The spacing corresponds to 150 n mi or 2.5 degrees in latitude. The spacing is one-half that in current use,

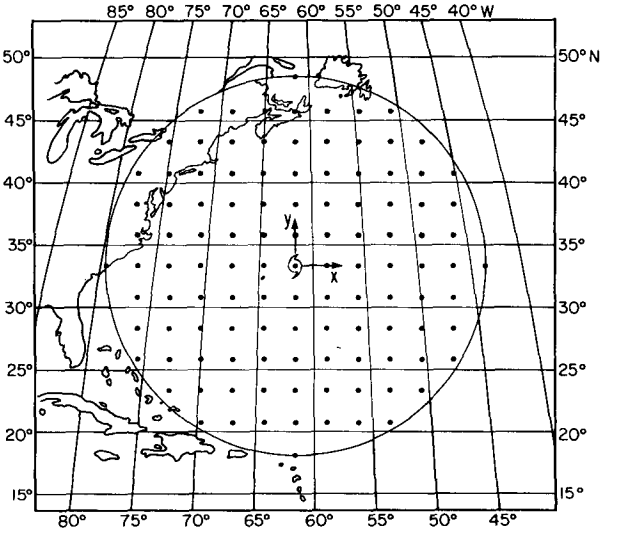

FIG. 2. Geographically-oriented grid system, centered on storm at 33°N, 61°W. Grid spacing is 278 km, measured along latitude and longitude circles.

and so allows better resolution of sharp gradients close to the storm center. The grid interval is consistent with the grid spacing of the large-scale analyses from which the grids are interpolated. There are 113 grid points within a circle of 1700 km radius. At this radius, the maximum distortion of the grid due to the convergence of meridians is only about 10% at 30°N. For a larger-scale grid, extending beyond 1700 km, a coordinate system based upon great-circle distances rather than latitude and longitude circles should be used. In the geographically oriented coordinate system, displacements relative to the storm center are positive in the eastward (x) and northward (y) directions.

To test the utility of reorientation of the coordinates with respect to storm heading, the height predictors are defined on a new grid, shown in Fig. 3. The grid is rotated so that it is oriented in the direction ϕ of the initial (time t_0) storm heading. For convenience this heading is determined by the difference between the $t_0 + 12$ h and $t_0 - 12$ h displacement vectors (see Fig. 3). The direction of this vector, determined from best-track positions, is a good approximation to the initial heading. The use of $t_0 \pm 6$ h positions instead to define the current heading would not give substantially different results. As discussed in Section 6, the results presented in this paper quantify the *potential* benefits that can be obtained from grid rotation with respect to a known (best-track) storm heading. Uncertainties in current storm position and heading will degrade an operational forecast.

Displacements are defined to be positive in the direction of the storm heading (y') and to the right (x'). Since the grid area is circular, the domain covered by the rotated and geographically-oriented systems is virtually the same. Thus, a direct comparison between the displacement errors associated with each system is possible. Moreover, a circular grid lessens the likelihood that corner predictors (typically not used) will fall outside the area of our dependent data.[1]

3. Distribution of displacement vectors

Storm displacement forecasts, made for 24, 48 and 72 h, are selected from 1421 available forecast situations at 0000 and 1200 GMT for all tropical storms and hurricanes in the North Atlantic basin from 1965 through 1980. Subtropical storms are included. Forecasts are not included in the developmental sample if any part of the 1700 km radius storm-centered grid (geographical or rotated) lies outside the NMC octagonal analysis (see footnote 1). Thus, storms initially south of about 25°N are excluded. For 24, 48 and 72 h, this restriction reduces the original 1421 cases to 795, 621 and 477, cases, respectively. Storm displacement forecasts are included for each prediction interval for which a best track position is available. Storms initially as far east as 15°W are contained in the sample, which includes storms that became extratropical or weakened below tropical storm strength (18 m s^{-1}) during the forecast interval. These forecast situations tend to be associated with larger than average displacements and forecast errors, but are relatively rare. For the 24 h prediction interval, the average initial storm position is 33.3°N, 61.6°W, as illustrated in Fig. 2. The average initial storm heading is 23° east of north, as illustrated in Fig. 3. Since storms south of about 25°N are excluded from the sample, the average tends to fall in the northeastward-moving post-recurvature part of the distribution of headings seen in Fig. 1.

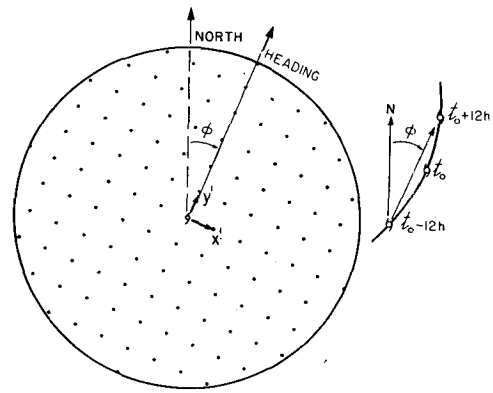

FIG. 3. Rotation of grid system with respect to storm heading. In this example, storm heading is $\phi = 23°$ (east of north). Curve to right of grid is storm track. Determination of heading ϕ at time t_0 from $t_0 - 12$ h to $t_0 + 12$ h storm positions is illustrated.

The forecast situation is depicted in Fig. 4a, which shows the distribution of observed 24 h displacement vectors in the geographically oriented system. There is one point for each of the 795 cases, with the arrow indicating the average vector displacement.[2] The dispersion of the points away from both coordinate axes is quite evident. The standard deviation of the eastward displacement (X) is $s(X) = 450$ km, which is of the same order as that for the northward displacement (Y), where $s(Y) = 348$ km. The total dispersion of the points is measured by the total variance $s^2(\text{tot}) \equiv s^2(X) + s^2(Y) = 323\,761$ km^2. The displacements along the forecast axes are not independent. The correlation between X and Y is $r(X, Y) = 0.45$. The combination of displacements in each coordinate direction into a vector displacement neglects the information contained in the dependence.

[1] Our grids are interpolated from the comparably-spaced NMC octagonal grid system, in use at NMC through 1974. Over the Atlantic area, the grid does not extend south of about 11°N.

[2] Since vectors rather than heading angles are averaged, the average vector displacement shown in Fig. 4a is not in the same direction as the average storm heading.

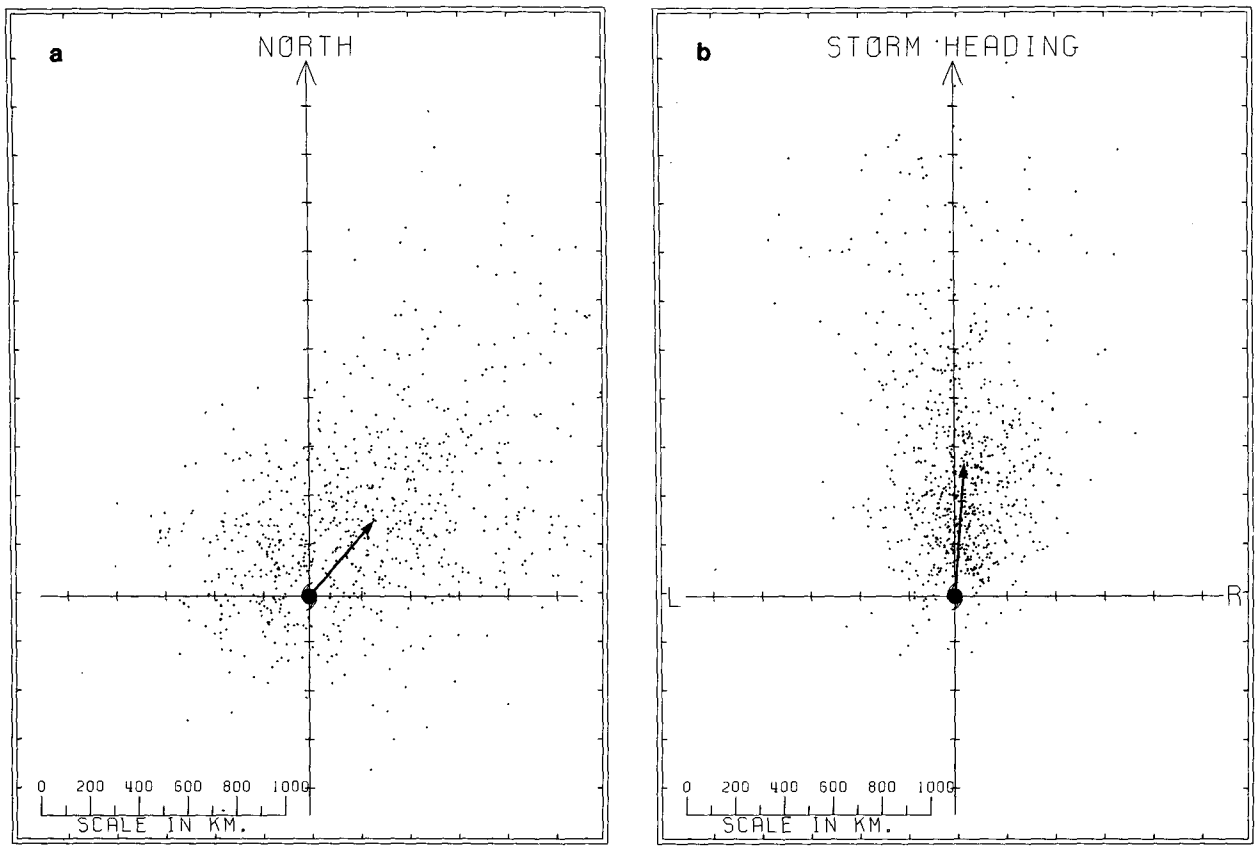

FIG. 4. (a) Distribution of tropical cyclone 24 h motion vectors for 795 cases from 1965–80 in geographically-oriented coordinate system. Top of figure points north. Arrow represents average vector displacement. (b) Same as (a) for coordinate system oriented with respect to storm heading. Top of figure points toward heading.

The effect of the rotation of the grid system with respect to initial storm heading is shown in Fig. 4b. In this case the points are clustered near the along-track (y') axis. The standard deviation in the cross-track direction, $s(X') = 163$ km, is much less than $s(Y') = 411$ km. The total variance $s^2(\text{tot}') = 196\,249$ km^2, which is only 60% of the variance in the geographical system. The goal of a forecast model is the reduction of the unexplained variance of storm motion. The task is made easier by rotation of the grid, which has the effect of reducing the variance that needs to be explained. Additionally, the correlation between displacements $r(X', Y') = 0.11$ in the rotated system. Unlike the geographical system, the two components are now nearly independent of each other. The two components in the rotated system may thus be separately forecast and then combined into a vector displacement.

The rotation of the grid system also has a beneficial impact on average speed error in a statistical track forecast model. Speed error is defined as the predicted minus observed magnitude of the total vector displacement, divided by the forecast time interval. Significant slow speed biases, averaging ~ 0.75 m s^{-1} have been reported for NHC73 (Neumann and Pelissier, 1981). By design of a statistical regression model the average bias of a scalar displacement is zero. Thus, if only one component (e.g., Y') were forecast and if all displacements were positive (so that $|Y'| = Y'$), then the speed bias would be zero. It is quite evident from a comparison of Fig. 4a and Fig. 4b that this limiting case is more nearly approached in the rotated system. Then, the variance of the cross-track component is small and the along-track displacements are all nearly positive. Thus, we expect 24 h speed biases to be greatly reduced when the rotated system is used. The potential improvement will be evaluated statistically in Section 4; the actual improvement cannot be evaluated until the model is employed in an operational rather than research mode.

Table 1 tabulates means ($\bar{X}$, $\bar{Y}$) and standard deviations [$s(X)$, $s(Y)$] of each component, and the standard deviation of the total displacement, s(tot), for 24, 48 and 72 h forecast intervals in both coordinate systems. The values for 24 h were discussed above. For 48 h, the fractional reduction of $s(X)$ from the geographical (X) to the rotated system (X') is much less than for 24 h; the reduction of the total variance is

TABLE 1. Distribution of displacements, hindcast skills, errors and speed errors for 24, 48 and 72 h forecasts using grid-point predictors. Both geographically-oriented and storm-heading coordinate systems are listed. $\bar{\mathbf{X}}$ is average displacement, and $s(\mathbf{X})$ is standard deviation of each component. s(tot) is total standard deviation (see text). m is number of predictors selected using 1% added reduction of variance cutoff; S_H is hindcast skill. For 24 h forecast, both cases with first two predictors chosen sequentially (seq.) and in pairs (pair) are shown. e_H is error, defined in text. Mean hindcast error (MHE) and speed error (MSE) are listed.

Forecast	Grid points	$\bar{X}$ (km)	$s(X)$	s(tot)		m	S_H	e_H (km)	MHE	MSE (m s^{-1})
					Geographical					
24 h	X	254	450	569	Sequence	4	0.746	308	258	−0.7
	Y	306	348			6	0.644			
	X				Pair	4	0.747	308	258	−0.7
	Y					5	0.646			
48 h	X	448	764	958	Sequence	3	0.527	676	567	−0.85
	Y	510	578			5	0.457			
72 h	X	638	1004	1255	Sequence	2	0.343	1016	860	−0.95
	Y	630	751			8	0.348			
					Rotated					
24 h	X'	39	163	443	Sequence	4	0.229	271	224	−0.25
	Y'	534	411			6	0.690			
	X'				Pair	3	0.205	278	232	−0.25
	Y'					3	0.669			
48 h	X'	172	497	849	Sequence	3	0.238	652	552	−0.6
	Y'	793	688			7	0.496			
72 h	X'	317	849	1240	Sequence	7	0.318	993	865	−0.8
	Y'	819	906			5	0.395			

also much smaller. For 72 h, rotation has little influence on the standard deviations of either the individual components or total displacement. For the longer forecast intervals the storm tracks have curved sufficiently that the coordinate orientation based upon initial motion is no longer appropriate. Thus, when 48 and 72 h forecasts are made, the advantages of grid rotation are substantially reduced or eliminated. The statistical results presented in Section 4 confirm this conclusion. The present analysis will concentrate on the potential improvements that can be made in short-range (~24 h) forecasts.

4. Screening of predictors: Forecast and speed errors

In order to quantify the effect of grid rotation on forecast errors and speed biases, deep-layer-mean height predictors are selected from the 113 available grid points using a step-wise screening technique (see, e.g., Draper and Smith, 1981) on each component separately. For 24 h forecasts, the first two predictors selected are those that explain the greatest fraction of the variance of storm motion, either sequentially (one at a time) or in pairs. The latter choice recognizes that storms are steered by winds that are associated with height gradients. These gradients are represented by two (or more) grid points. Fig. 5 shows the correlation between the heights and the components of the 24 h displacement in the geographically-oriented system. The correlation fields are oriented at an angle to the coordinate directions. In particular, the correlation field for northward displacement (Fig. 5b) is oriented in nearly the direction of the average 24 h displacement. The positions of the first two grid points selected in the screening of predictors are also indicated. In general, the paired predictors tend to lie closer to the center of the grid than their sequentially-chosen counterparts, and are more symmetrically placed with respect to the forecast axis.

In contrast to Fig. 5, the correlation fields in the rotated grid system (Fig. 6) are aligned nearly along the respective coordinate axes. As before, the paired predictors tend to lie closer to the center of the grid. The symmetry of paired predictors with respect to the along-track axis in Fig. 6b is striking. The predictors both lie one grid point ahead, and three grid points to the left or right of the storm center. The positioning of the predictors ahead of the storm is physically reasonable, since the gradient ahead of the storm is representative of the winds in the region where the storm is moving during the forecast interval. The average 24 h storm displacement is about 540 km. Gradients ahead of the storm by half this distance, 270 km, will be representative of the average wind that steers the storm

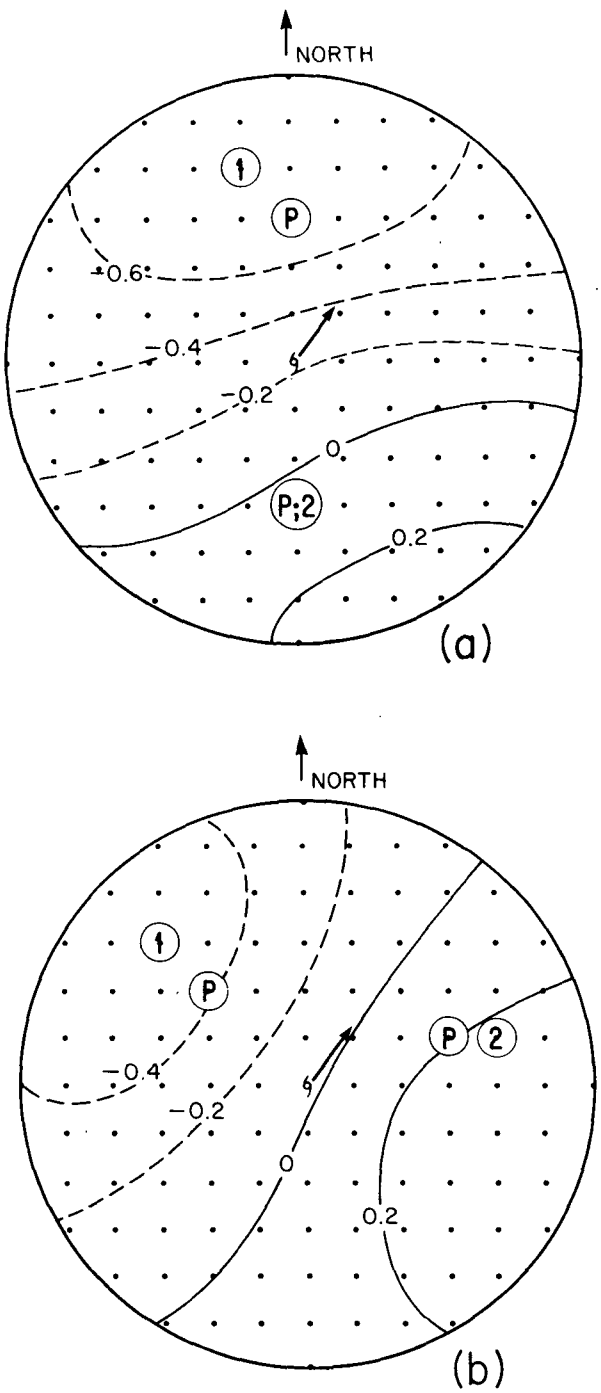

FIG. 5. Correlation coefficient between height field in geographically oriented system and 24 h (a) eastward and (b) northward storm displacement. The maximum correlations are −0.76 and −0.49, respectively. The circled numbers indicate, in order, the sequentially selected predictors; the letter P indicates the predictors selected in pairs. The arrow designates the average vector displacement.

during the 24 h interval. This distance is approximately one grid point, the actual distance of the paired predictors ahead of the storm. The distance between the paired predictors and along-track axis is explained in the following section. The orientation of the correlation fields along the forecast axes, and the symmetry of the

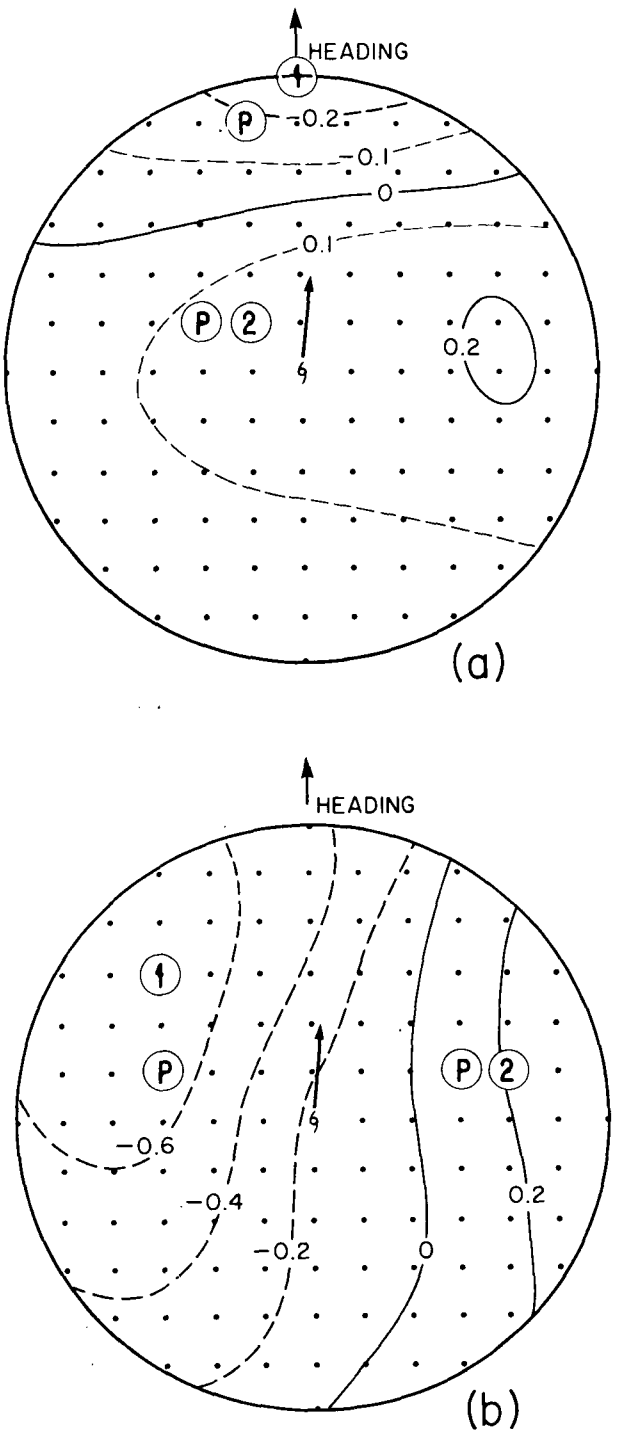

FIG. 6. As in Fig. 5, for rotated coordinate system and (a) cross-track and (b) along-track displacements. Maximum correlations are −0.27 and −0.69, respectively.

paired predictors about the axes, reemphasizes the independence of the components of storm displacement in the rotated system. Along-track winds tend to produce along-track motion, which is essentially uncorrelated with cross-track motion.

The step-wise screening algorithm was continued until the added reduction of variance due to one additional predictor was less than 1%. This cutoff is a traditional one, and was used in the development of some earlier empirical and statistical track forecast models. The total number of predictors (m) selected for each component and the total fractional reduction of variance, or hindcast skill, S_H (cf. Davis, 1977), are given in Table 1. Results are shown for 24 h, with the first two predictors selected sequentially or in pairs, and for 48 and 72 h forecasts (sequential only). A maximum of eight predictors is selected for a given component. For 24 h there is little difference between skills for the sequential and paired selections. The skill in predicting the cross-track component is small, with $S_H \approx 0.2$.

The component predictions are combined to give a forecast of vector displacement. Two measures of average displacement error are given in Table 1. The *mean hindcast error* (MHE) is the average of the distances between the predicted and observed storm positions at the end of the forecast interval. This quantity has been previously referred to as the mean vector error or mean forecast error (Neumann and Pelissier, 1981). The quantity e_H is the square root of the sum of the mean square displacement errors (predicted minus observed) for both displacement components. This quantity is the combined standard error for both components. When $S_H = 0$ for each component, $e_H = s(\text{tot})$. It is easily shown that the MHE is always $\leq e_H$, which is seen in Table 1.

The term hindcast and subscript H are used here to emphasize that the reduction of variance (skill) and errors are computed from the developmental set of data. Due to random errors, the regression equations derived from these data will not perform as well in a forecast, giving smaller skills and larger errors (cf. Davis, 1977). Using a Monte Carlo significance test, Neumann *et al.* (1977) found that the traditional 1% added reduction of variance cutoff was too lax. In order to achieve high statistical reliability, in general fewer predictors should be retained. Their analysis was not used, however, in the formulation of NHC73 (Neumann and Lawrence, 1975), which probably contains too many predictors. Neither the statistical significance of predictors nor the actual forecast skill or errors are considered in the present analysis. It will be shown in a future paper that the use of more stringent significance levels does reduce the number of predictors accepted, but does not have a very large effect on the actual forecast skill.

For the 24 h forecast, rotation of the grid with respect to storm heading reduces the error (MHE or e_H) by about 13%. This reduction by itself is comparable to the decrease in actual official forecast errors from 1954–1980. The MHE decreases from about 260 km to about 225 km. The combined hindcast skill for both displacement components together is measured by $\{1 - [e_H/s(\text{tot})]^2\}$. This quantity is 0.71 in the geographically-oriented system and 0.63 in the rotated system. Thus, the fractional reduction of total variance is slightly greater for the geographical than the rotated system. Due to the much smaller variance $s^2(\text{tot})$ in the latter case, however, the combined standard error e_H is also smaller in the rotated system. Thus, the rotated grid system has a greater potential for the reduction of forecast errors. The *mean speed error* (MSE), given in the last column of Table 1, decreases by a factor of about ⅔ from -0.7 m s^{-1} to -0.25 m s^{-1}. Negative values indicate a slow bias. Thus, for short-range forecasts the grid rotation has the potential for substantially reducing both the forecast error and slow bias found in the geographically oriented system. For 48 h, the reduction is substantially diminished. The MHE and e_H decrease by only a few percent. For 72 h, the reduction is essentially eliminated; the MHE actually increases slightly, while the MSE is reduced by only a few percent. These results confirm the analysis in Section 3 that considered differences between the distributions of storm displacement vectors in the two coordinate systems.

The size of the grid needed to represent synoptic data depends on the length of the forecast period. For a 24 h forecast, a grid extending outward no more than 1000 km can be used, since almost all the predictive information lies within that radius. The location of the predictors selected in the present study, the first two of which (shown in Figs. 5 and 6) provide the major portion of the total variance, supports this statement. Recent studies at NHC indicate that the contribution of predictors outside 1700 km to a 24 h forecast is small. For 48 and, especially, 72 h, some predictive information may be present outside this radius. Thus, for longer-range forecasts a large-scale grid such as that shown in Fig. 3 of Neumann and Lawrence (1975) should be used. Due to the limited size of the grid in the present analysis, the large-scale predictors are not available. The values of hindcast skill could be slightly increased (and errors reduced) by admission of these additional predictors. Some independent analyses (not shown) indicate, however, that predictors outside the 1700 km radius grid are replaced, in the present analysis, by additional predictors selected *within* the grid. In any case, the skills and errors can be compared, in a relative sense, between the rotated and geographically-oriented systems. For 24 h forecasts grid rotation has a potentially substantial beneficial effect on prediction; for 48 and 72 h the effect is either diminished or eliminated, due to the change in storm heading during the forecast interval. The following section focuses on the predictors of 24 h motion.

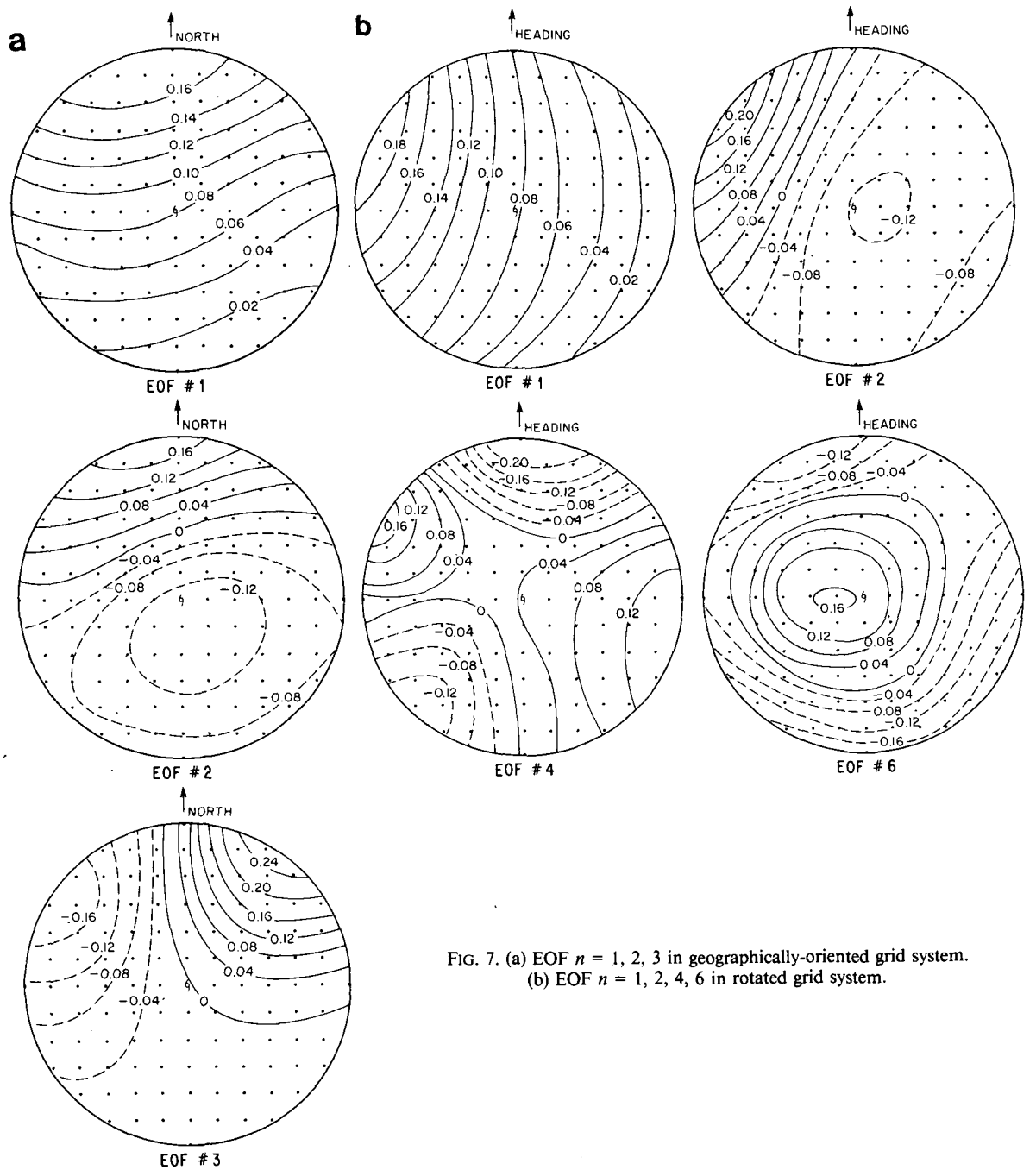

FIG. 7. (a) EOF n = 1, 2, 3 in geographically-oriented grid system. (b) EOF n = 1, 2, 4, 6 in rotated grid system.

5. Model development in terms of EOFs and PEPs

The geopotential height data used in this study have been defined on a 113 point storm-centered grid. In the previous section, the individual grid points were made available to the screening program for the development of regression equations that predict storm displacement. An alternate representation of the height data can be made in terms of Empirical Orthogonal Functions (EOFs). These functions, discussed in Appendix B of Davis (1976), form an efficient representation of the data field for use in statistical prediction. The modes are uncorrelated, and are ordered with respect to their contribution to the total variance in the data, the first mode explaining the greatest portion of the variance. In the present case the first 10 EOFs alone, either in the rotated or geographically oriented systems, explain about 98% of the total height variance. Selected EOFs (designated by their mode numbers n) are shown in Fig. 7 for both the rotated and geograph-

ical systems. The 24 h hindcast skills, using the first 10 EOFs as predictors, are shown in Table 2. They are very close to those derived from the screening of grid-point predictors (Table 1), with the first two predictors chosen sequentially. Differences between the grid-point and EOF predictors in actual forecast skill will be considered elsewhere.

The reduction of variance in the 24 h displacements is distributed among the 10 EOFs. The EOFs that contribute the most substantial part of the reduction of variance for the individual components are listed in Table 2, together with their fractional contribution to S_H (in % of S_H). Fig. 7 includes all EOFs that are listed. The coupling of the eastward (X) and northward (Y) predictions in the geographically-oriented system, noted in Sections 3 and 4, is evident in the large contribution of EOF $n = 2$ to both components. By contrast, EOFs contributing to along-track (Y') predictions (rotated EOF $n = 1$ and 2) do not contribute to cross-track prediction, and vice versa.

Since there are two predictands, the components of the displacement, and several EOFs contributing to the prediction of each component, it is difficult to visualize the relationship between the height predictors and the displacements that they predict. A convenient method for combining EOFs into a compact representation that allows easy interpretation is formulated by Davis (1977). The method is to develop new uncorrelated data patterns, called Principal Estimator Patterns (PEPs), that are ordered according to their contribution to the variance in the predictand field, which here is the two-component vector displacement. For example, the first height PEP ($n = 1$) predicts the greatest possible part of the total variance s^2(tot). The associated vector $\mathbf{X} = \mathbf{d}_1$ is the displacement predicted by this PEP. Details of the method are described by Davis (1977, 1978). The height PEPs, and the vector displacements $\mathbf{d}_n$ that they predict, are shown in Figs. 8 and 9. The length of $\mathbf{d}_n$ is the standard deviation of the displacement explained by the nth PEP. The sign of the PEP is arbitrary; if the sign reverses, the direction of $\mathbf{d}_n$ also reverses. Since there are two displacement components, there are only two PEPs.

TABLE 2. Hindcast skills (S_H) for 24 h forecasts using $m = 10$ EOFs. Largest EOF mode (n) contributions are listed (in % of S_H).

		m	S_H	Dominant EOF contributions	
			Geographical		
24 h	X	10	0.749	$n = 1$ (57%)	$n = 2$ (33%)
	Y	10	0.646	$n = 3$ (40%)	$n = 2$ (21%)
			Rotated		
24 h	X'	10	0.235	$n = 4$ (36%)	$n = 6$ (31%)
	Y'	10	0.687	$n = 1$ (49%)	$n = 2$ (33%)

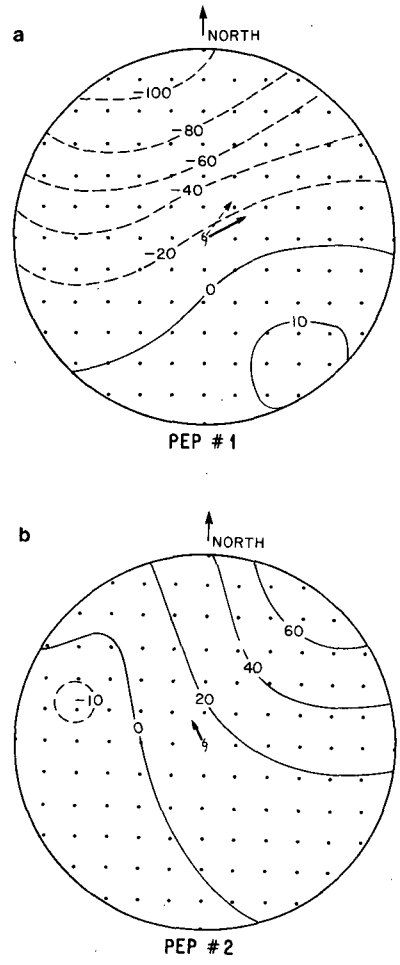

FIG. 8. (a) PEP $n = 1$ for 24-h storm motion in geographically-oriented grid system (in meters). Solid vector is $\mathbf{d}_1$, the displacement predicted by this PEP. Dashed vector is average 24 h displacement. (b) Same as Fig. 8a, but for PEP $n = 2$ and $\mathbf{d}_2$.

In both coordinate systems, the height PEPs are oriented nearly along $\mathbf{d}_n$, the displacements that they predict. The vectors $\mathbf{d}_n$ point very nearly in the directions of the axes along which the components of the displacements are independent (uncorrelated). The near coincidence of $\mathbf{d}_1$ with one of the axes of independence indicates that predictions are best for displacements along this axis, which is in the direction that maximizes the variance in a single component. In the geographically-oriented coordinate system (Fig. 8), this axis is at a substantial angle from the coordinate axes. Also, the direction of the average 24 h displacement is seen to lie at an angle with $\mathbf{d}_1$. Fig. 4a indicates that the dispersion of displacement vectors about this average is substantial. Thus, predictions in the geographically-oriented system are not optimized. As was demonstrated in Section 3, the role of rotation of the coordinate system with respect to storm heading is to

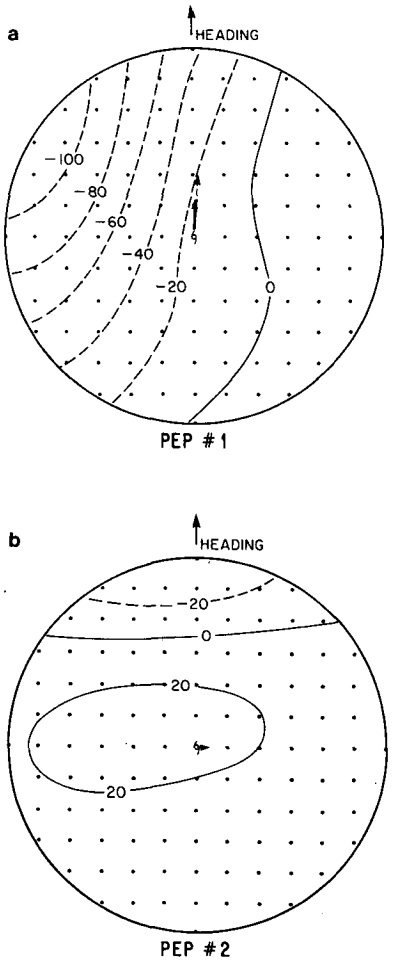

FIG. 9. (a) As in Fig. 8 but for rotated coordinate system.

maximize the variance in one displacement component (along-track), and thereby produce nearly independent forecast axes. Then $\mathbf{d}_1$ is nearly coincident with the along-track axis (Fig. 9). The dispersion of displacements about that axis is small (Fig. 4b), so that displacement predictions are nearly optimum. The resemblance between the PEPs in Fig. 9 and the correlation fields in Fig. 6 emphasizes the independence of the components of displacement in the rotated system. Rotated PEP $n = 1$ corresponds to Fig. 6b, and $n = 2$ to Fig. 6a. By contrast, there is no corresponding correlation field in Fig. 5 corresponding to PEP$n = 2$ in Fig. 8b. Although, as noted in the discussion of Fig. 7 and Table 2, EOF $n = 2$ has a substantial contribution to the prediction of both displacement components in the geographical system, this EOF has very little weighting in PEP $n = 2$. The PEP formulation decouples the forecast components in the geographical system.

The PEP $n = 2$ in Fig. 9b represents the height distribution that most efficiently predicts displacements in the direction of $\mathbf{d}_2$. This direction is essentially the cross-track component. Thus, one would expect the height pattern to be associated with storm turning motion. There is, in fact, a considerable resemblance between this PEP and the 500 mb composite streamline patterns for left- or right-turning storms shown in Fig. 9 of Chan *et al.* (1980). The present analysis confirms the relation between the flow ahead and within 1700 km of the storm center with short-term future cross-track motion. A reduction of variance of only about 20% is found, however, indicating little predictive skill for the small 24 h cross-track component.

Another set of EOFs and PEPs can be developed in terms of height predictors normalized by the standard deviation at each individual grid point. This normalization equalizes the contribution of each point to the total height variance. In that case, the first PEP in the rotated system (not shown) predicts the along-track component. This PEP is nearly proportional to the correlation fields in Fig. 6b. It is comprised primarily of EOF $n = 2$, shown in Fig. 10. The height distribution of this normalized EOF provides insight into the position of the paired grid point predictors that best predict along-track motion (cf. Fig. 6b). For clarity these predictors are shown in Fig. 10. As noted in Section 4, the predictors lie one grid point (24 h displacement/2) ahead of the storm center. At this distance ahead of the storm, the height gradient in Fig. 10 across the storm track is nearly uniform out to a distance of about three grid points from the along-track axis. This distance is one-half the separation of the paired predictors. At larger distances from the along-track axis, the gradient weakens. At small distances, the gradient remains the same but the amplitude of the EOF decreases. Thus, the six grid-point separation of the paired

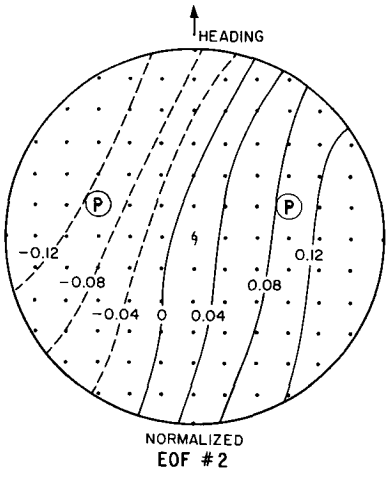

FIG. 10. EOF $n = 2$ in rotated coordinate system, with grid-point height predictors normalized with respect to their standard deviations. Letters P are paired predictors selected by screening regression.

predictors effectively represents the normalized EOF $n = 2$. This EOF dominates the composition of PEP $n = 1$, which mirrors the correlation fields for along-track prediction.

6. Discussion

Tropical storms tend to move with the surrounding synoptic flow, and have a very strong persistence in their motion. Thus, a grid system oriented with respect to storm heading is a natural one. Forecast errors for prerecurvature storms south of 25°N, not included in the developmental sample, are typically smaller than those for post-recurvature storms. Moreover, the heading of these storms tends to fall in the west-northwestward part of the distribution seen in Fig. 1, and to be more nearly aligned with a latitude–longitude grid. Thus, grid rotation is likely to reduce the forecast error less for lower-latitude storms than for the sample presented here. Similarly, in the extreme cases of substantial changes in heading during 24 h (cf., Fig. 4b), grid rotation will have a relatively small beneficial impact. Forecast systems that depend on geographically-oriented climatological flow patterns would not be expected to be benefited by storm-heading oriented systems.

We have found that a potential reduction of 24 h forecast errors by about 13% could be realized for synoptic predictors developed on the rotated grid. This reduction is comparable to the entire reduction in 24 h operational forecast errors during the past 25 years. Since there is such a strong persistent component to the motion, the extraction of any additional information from synoptic steering predictors is significant. The short-range ($\leq$36 h) forecast is the most critical time interval for warnings of land-falling storms. Even a small reduction of error is important. The substantial reduction in slow speed bias by a factor of ⅔ is a related benefit of the reoriented coordinate system.

Other investigators have used EOFs as an alternative to grid-point predictors in tropical cyclone forecast models (Shaffer and Elsberry, 1982). In the present study, their use together with PEPs provided an interpretation of both the role of grid rotation in the improvement of forecasts, and the position of grid-point predictors. Forecasts are optimized in the direction along which the variance in storm motion is maximized. Rotation tends to orient storm displacement vectors along this (along-track) direction. The cross-track separation of the paired grid-point predictors effectively represents the normalized EOF that best predicts along-track motion. A topic of current investigation is a comparison of the actual forecast (as opposed to hindcast) skills and errors of the grid-point and EOF models.

Due to random and real errors present in the developmental and operational height data, respectively, the entire reduction in error found in this analysis will not be realized. The effect of random errors on actual forecast skill will be presented in a future paper. Initial storm positioning errors will also have an adverse effect on the forecasts. The uncertainties in the current storm position lead to uncertainties in the initial storm motion. These uncertainties directly degrade all statistical and dynamical forecast models, which use the initial storm motion to extrapolate future storm track. The rotation of the grid system with respect to storm heading introduces an additional indirect effect. If the storm heading is in error, the orientation of the grid will be offset relative to the actual motion vector. This offset will give a larger apparent cross-track component to the short-range motion, which will be correlated with the along-track displacement. Thus, the forecast will be degraded.

As we have emphasized, the results given in this paper represent the potential forecast improvement that can be made in short-term forecasts with current synoptic data if the storm heading is known. Further research is needed to determine whether continuous rotation of the grid system, with respect to known future motion, could assist in longer-range forecasts. The ideas presented must still be tested in an operational environment. Such tests are currently being made. Even if operational implementation indicates that there is no actual improvement in forecast ability, however, the results give strong incentive both for improved operational storm center fixes to define the storm heading and improved observations of winds in the vicinity of the storm to define the steering flow. Only in this way will the statistical short-range track forecast be substantially enhanced. The 13% error reduction, which is a limiting case for a 24 h forecast, can be approached as knowledge of current motion is improved. An omega-dropsonde program of the Hurricane Research Division, first employed during the 1983 hurricane season, is explicitly designed to fill in the data void in the vicinity of the storm, especially at middle levels. Satellite data will also help fill the void.

Acknowledgments. The authors wish to thank Ms. Angel Tillman for typing the manuscript, and Mr. Dale Martin for drafting the figures. Ms. Mary A. Davis assisted in the preparation of the distribution of cyclone motion vectors.

REFERENCES

Chan, J. C. L., W. M. Gray and S. Q. Kidder, 1980: Forecasting tropical cyclone turning motion from surrounding wind and temperature fields. *Mon. Wea. Rev.*, **108**, 778–792.

Davis, R. E., 1976: Predictability of sea-surface temperature and sea-level pressure anomalies over the North Pacific Ocean. *J. Phys. Oceanogr.*, **6**, 249–266.

——, 1977: Techniques for statistical analysis and prediction of geophysical fluid systems. *Geophys. Astrophys. Fluid Dyn.*, **8**, 245–277.

——, 1978: Predictability of sea level pressure anomalies over the North Pacific Ocean. *J. Phys. Oceanogr.*, **8**, 233–246.

Draper, N. R., and H. Smith, 1981: *Applied Regression Analysis*, 2nd ed., Wiley, 709 pp.

George, J. E., and W. M. Gray, 1976: Tropical cyclone motion and surrounding parameter relationships. *J. Appl. Meteor.*, **15**, 1252–1264.

Miller, B. I., and P. L. Moore, 1960: A comparison of hurricane steering levels. *Bull. Amer. Meteor. Soc.*, **41**, 59–63.

Neumann, C. J., 1978: Comments on "Tropical Cyclone Motion and Surrounding Parameter Relationships." *J. Appl. Meteor.*, **17**, 418–419.

——, 1981: Trends in forecasting the tracks of Atlantic tropical cyclones. *Bull. Amer. Meteor. Soc.*, **62**, 1473–1484.

——, and M. B. Lawrence, 1975: An operational experiment in the statistical-dynamical prediction of tropical cyclone motion. *Mon. Wea. Rev.*, **103**, 665–673.

——, —— and E. L. Caso, 1977: Monte Carlo significance testing as applied to statistical tropical cyclone prediction models. *J. Appl. Meteor.*, **16**, 1165–1174.

——, and J. M. Pelissier, 1981: Models for the prediction of tropical cyclone motion over the North Atlantic: An operational evaluation. *Mon. Wea. Rev.*, **109**, 522–538.

Sanders, F., A. C. Pike and J. P. Gaertner, 1975: A barotropic model for operational prediction of tracks of tropical storms. *J. Appl. Meteor.*, **14**, 265–280.

Shaffer, A. R., and R. L. Elsberry, 1982: A statistical-climatological tropical cyclone track prediction technique using an EOF representation of the synoptic forcing. *Mon. Wea. Rev.*, **110**, 1945–1954.